12th International Symposium on Turbulence and Shear Flow Phenomena (TSFP12)
Osaka, Japan, July 19–22, 2022

# EXPERIMENTAL STUDY ON A TRANSITION OF FLOW IN WEAKLY UNSTABLY STRATIFIED TURBULENT BOUNDARY LAYERS

**Yoshinori Mizuno*, Toshimasa Yagi and Kazuyasu Mori**
Meteorological Research Institute
Nagamine 1-1, Tsukuba, Ibaraki, Japan
*ymizuno@mri-jma.go.jp

## ABSTRACT

We investigate the dependence of turbulence statistics and structures in weakly unstably stratified turbulent boundary layers through wind-tunnel experiments. In the constant-flux layer where some universal properties of turbulence such as a similarity of turbulent statistics are expected to be observed, the production rate of turbulent kinetic energy due to shear increases at large scales comparable to the boundary layer thickness $\delta$ with the relative strength of buoyancy effect, evaluated by $-\delta/L$ where $L$ is the Obukhov length. It is found that the vertical profile of the variance and spectrum of the streamwise velocity component are not modified by the stratification up to $-\delta/L \approx 1$. On the other hand, they exhibit a drastic change beyond $-\delta/L = 1$, that is likely to be attributed to a transition in the flow structures due to the buoyancy effect. The two-point correlation functions of horizontal velocity fluctuations indicate the emergence of roll-like vortical structures for $-\delta/L > 1$.

## INTRODUCTION

In an unstably stratified boundary layer, both shear and buoyancy effects contribute to the production of turbulent kinetic energy. According to a dimensional analysis (Monin & Obukhov, 1954), the turbulence statistics measured at the wall-height $z$ is parameterized by $z/L$, where $L \equiv -u_*^3\Theta/\kappa g Q_0$ is the Obukhov length, and $u_*$ is the friction velocity, $Q_0$ is the temperature flux on the wall, $g$ is the gravitational acceleration, and $\Theta$ is a representative temperature in the boundary layer. Since $Q_0$ is defined to be positive when the flux is upward, $L$ is negative for unstably stratified cases. The absolute value $|L|$ is interpreted as the height at which the effect of buoyancy becomes important (Wyngaard, 2010). The ratio $z/|L|$ measures the local strength of stratification at the height $z$, while $\delta/L$ where $\delta$ is the boundary layer thickness measures the global strength of stratification throughout the boundary layer.

It is widely known that streamwise rolls spanning almost full height of the boundary layer appear under weakly unstable stratification (Etling & Brown, 1993). Due to the presence of such large-scale rolls, streamwisely long stripes of upward and downward motions along the rolls are observed, and they are responsible for the vertical transfer of momentum, heat and so on. Detailed and systematic studies on the structures in a turbulent boundary layer parameterized by the stability parameter $\delta/L$ or $z/L$ are rarely found. Among them, a recent direct numerical simulation (Pirozzoli *et al.*, 2017) of a horizontal channel under unstable stratification showed that streamwise rolls appear for $-\delta/L$ up to $O(1)$. Blass *et al.* (2020) also pointed out that the buoyancy effect emerges after $L$ excesses a factor of the system size. While it is still difficult for direct numerical simulations to achieve high Reynolds numbers encountered in engineering and nature, laboratory experiments have a relative advantage to attain a higher Reynolds number and to acquire long-time measurements. We perform an experimental study on the transition of flow structures caused by the rise of buoyancy effect in weakly stratified boundary layers.

## EXPERIMENTS

The data set for the present analyses was generated from experiments in an open-return wind tunnel at Meteorological Research Institute, located at Tsukuba, Japan. The test section is a uniform rectangular duct, which is 18 m long, 3 m wide, and 2 m high. Aluminium rods with a diameter of 3 mm were placed at intervals of 100 mm on the floor to create rough surface throughout the test section. The rectangular cross-section with the same dimensions extends 4 m upstream from the test section, and the rods were also placed within this part in the same manner. Measurements were performed 14 m downstream from the entrance of the test section by a laser-Doppler velocimeter (LDV, Dantec model F60 with 60X17). Its sensing volume has a diameter of 120 $\mu$m and length of 1.5 mm oriented in the spanwise direction. A boundary layer was formed by blowing air at a constant speed into the test section, and the streamwise and wall-normal velocities were measured at different heights along a traverse through the boundary layer. Since the signals of the two velocity components were recorded independently, their time-sequences were resampled for synchronization to evaluate their cross-correlation.

Unstable stratification was generated by heating the floor of the test section. The temperature of the floor was controlled so that its difference from that of incoming air is constant. The thermal flux $Q_0$ on the floor was measured by two plate-type heat flow sensors (Eto-denki, M55A). Each has the dimensions of $50 \times 50 \times 0.7$ mm. On the floor, they are mounted up- and downstream sides of an aluminium rod under the LDV probe. The boundary layers discussed in this paper are summarized in Table 1. Figure 1 shows two examples of visualization of neutral (N) and unstable (U3) boundary layers. In the unstable case in 1(b), we can recognize some tall vertical fluid motions which is absent of the neutral case in 1(a). We will show how turbulence statistics are modified by the emergence of such buoyancy-driven motions.

We also obtained two-dimensional velocity fields in a horizontal plane by a Particle Image Velocimetry (PIV) technique (Flowmap, Dantec Dynamics A/S). The measurement field of view is 496 mm long and 397 mm wide for all the cases. Statistics for each case are compiled from 9000 (N), 6600 (U2) or

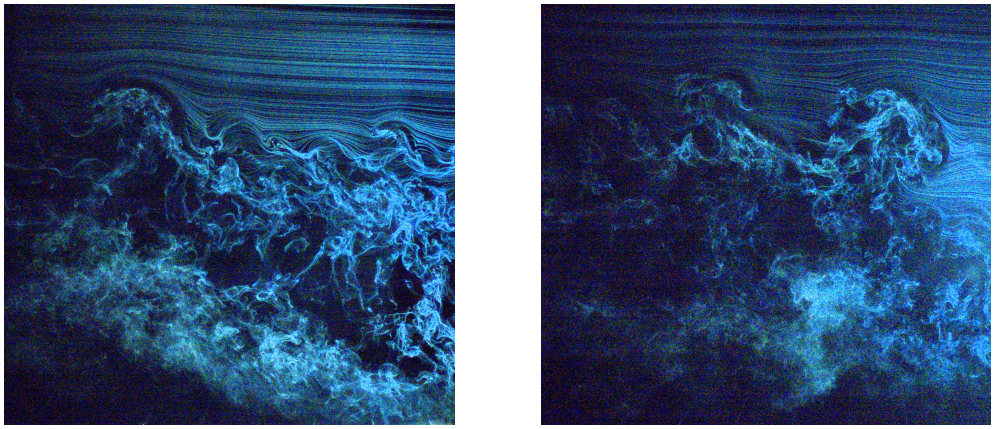

(a) (b)

Figure 1. Turbulent boundary layers (a) neutrally stable and (b) unstable at $-\delta/L = 2.6$ visualized by smoke-wire in a wind tunnel. The air flows from right to left.

2300 (U3) images obtained at the sampling rate of 0.5 Hz.

Hereafter the streamwise, spanwise and wall-normal (vertical) coordinates are denoted by $(x,y,z)$, and velocity fluctuations by $(u,v,w)$ in these directions, and an overline stands for averaging in time.

Table 1. Parameters in the present boundary layers. Here $U_\infty$ is the free-stream velocity, $\Delta\Theta$ is the temperature difference between the incoming air and floor, and $Re_\tau$ is the friction Reynolds number.

| | $U_\infty$ [m/s] | $\Delta\Theta$ [K] | $Re_\tau$ | $-\delta/L$ | Symbol |
|---|---|---|---|---|---|
| N | 1.5 | - | 2380 | – | × |
| U1 | 3 | 20 | 4620 | 0.43 | ▲ |
| U2 | 2 | 20 | 3760 | 1.2 | ● |
| U3 | 1.5 | 20 | 3810 | 2.6 | ● |

## RESULTS

The profiles of some one-point statistics in the present boundary layers are shown in figure 2. We here use $u_* = \sqrt{-\overline{uw}}$ within the vertical range where the momentum flux is constant, so called constant-flux layer, as a velocity scale. This gives a good approximation for the friction velocity, though not discussed in detail here. For all the boundary layers realized in the present experiments, the layer is indeed found up to $z/\delta \approx 0.2$, as shown in figure 2(b).

Figure 2(a) compares the mean streamwise velocity $U$ for different values of $\delta/L$. The profiles are expected to collapse to the neutral case near the wall where the effect of shear is dominant against the stratification, and start diverging as the height $z$ increases. The effect of stratification apparently emerges gradually on the mean velocity profile as $-\delta/L$ is increased.

The profiles of the variance $\overline{u^2}$ and covariance $\overline{uw}$ are shown in figure 2(b). For the neutrally stable case, a logarithmic dependence of the variance $\overline{u^2}$ of the streamwise velocity fluctuation was predicted and supported by experiments (Townsend, 1976; Marusic *et al.*, 2013). As in the figure, the variance does not show any clear dependence on the stability parameter up to $-\delta/L \approx 1$, but the most unstable case (U3) obviously deviates from the other cases, implying a transition of the flow by increasing the stability parameter $-\delta/L$ beyond $-\delta/L \approx 1$. In that case, the variance $\overline{u^2}$ and covariance $\overline{uw}$ (and also $\overline{w^2}$ though not shown here) have the second peak in their magnitude in the outer layer, at $z/\delta \approx 0.5$. At this location, corresponding to $-z/L \approx 1$, the buoyancy effect explicitly emerges in those profiles.

The vertical momentum flux $\overline{uw}$ and also production-rate of turbulent kinetic energy $-\overline{uw}dU/dz$ are enhanced by unstable stratification at large scales comparable to $\delta$, as shown in figure 3(a), but gradually even for $-\delta/L < 1$ where variances are not modified. The peak is located at $\lambda/\delta \approx 5$ for all the unstable cases, and it seems not dependent of the height $z$ neither. The enhancement of momentum flux is observed only at large scales (Mizuno *et al.*, 2022), but it does not modify the structure of $u$ for $-\delta/L$. As expected from the behavior of the variance, the spectrum of $u$ shown in figure 3(b) is robust up to $-\delta/L \approx 1$, and again drastic change occurs when $-\delta/L$ is further increased. The mechanism of energy transfer at least for the streamwise velocity component in the neutral case is retained up to $-\delta/L \approx 1$, and the buoyancy effect contributes only to increasing the energy production and does not affect the flow structures.

To examine the buoyancy effect on flow structures, a large amount of snapshots of the two-dimensinal velocity field on a horizontal plane obtained by PIV are compiled to the two-point correlation function of velocity fluctuations, defined by

$$C_{\alpha\alpha}(r_x.r_y) \equiv \frac{\overline{\alpha(x+r_x,y+r_y)\alpha(x,y)}}{\sqrt{\overline{\alpha(x+r_x,y+r_y)^2}}\sqrt{\overline{\alpha(x,y)^2}}},$$

where $\alpha = u$ or $v$. Though the length of the measurement field of view is comparable, or even shorter than $\delta$, it is confirmed that the functions for the neutral case N agree well with a DNS by Sillero *et al.* (2014), at least, for $r_x$ and $r_y$ within the ranges of the field of view. The effect of unstable stratification on the correlation functions are here presented at $z/\delta \approx 0.15$. Figure 4(a) shows that $u$ has a longer correlation length in the streamwise direction for the unstable cases U2 and U3, which seems to be attributed to the emergence of roll-like vortical structures in these cases. For the neutral case, the streamwise velocity

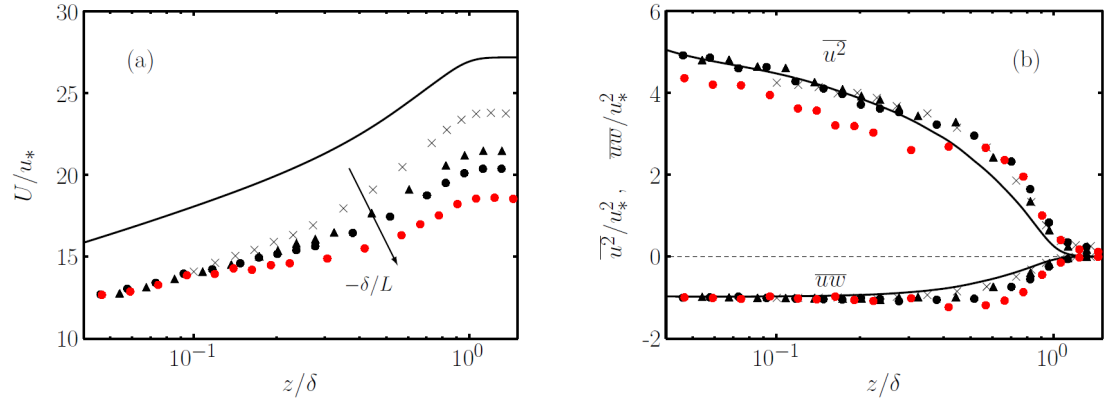


Figure 2. Vertical profiles of (a) the mean streamwise velocity $U$ and (b) Reynolds stresses $\overline{u^2}$ and $\overline{uw}$. Symbols are as in Table 1. The solid lines are the profiles in a DNS of a neutrally stable case for $Re_\tau = 1999$ by Sillero *et al.* (2013).

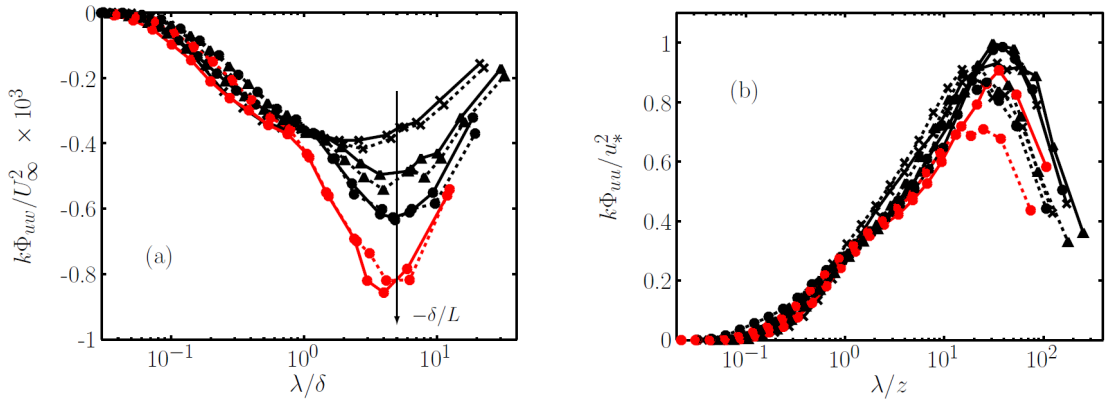


Figure 3. (a) Cospectrum of $u$ and $w$ and (b) spectrum of $u$ as functions of the streamwise wavelength $\lambda$ at $z/\delta = 0.12$ (solid) and 0.18 (dashed). Symbols are as in Table 1.

fluctuations at two separate locations in the spanwise direction within a certain range correlate negatively to each other. This negative correlation is preserved under unstable stratification in the present cases, as shown in figure 4(b). Though not shown here, the negative peak of correlation locates at $r_y/\delta \approx 0.4$, irrespectively of the value of $\delta/L$ and the height of $z$ for the unstable cases. The negative correlation is therefore associated to $\delta$-scaled large scale structures.

The effect of unstable stratification is also observed in $C_{vv}$. As seen in figure 5(a), the positive correlation becomes stronger, and correlation length in the streamwise direction is elongated as $-\delta/L$ increases. For the spanwise distance, as shown in figure 5(b), only the most unstable case U3 significantly deviates from the others, and gives a longer correlation length. Furthermore, $C_{vv}(0, r_y)$ at $r_y/z = 5$ is found to be slightly negative for the unstable cases. The both correlation lengths in the $x$ and $y$ directions of $v$ become longer by the buoyancy effect. These observation also evidence the emergence of coherent roll-like structures.

## CONCLUSIONS

It is found that the vertical profile of the variance and also spectrum of the streamwise velocity component are not modified by the stratification up to $-\delta/L \approx 1$. This indicates that the mechanism of energy transfer of the streamwise velocity component in a neutral case is retained in that range of $-\delta/L$. On the other hand, they exhibit a qualitative change beyond $-\delta/L = 1$, that is likely to be attributed to a transition in the flow structures due to the buoyancy effect on the flow. The two-point correlation functions of horizontal velocity fluctuations also indicate the emergence of roll-like vortical structures for $-\delta/L > 1$.

Our present measurements can extract only a portion of full information on the flow, that is not enough for comprehensive understanding of flow structures in stratified boundary layers. In addition, the present range of $\delta/L$ probably reaches only the beginning of the transition toward the buoyancy dominat regime (Blass *et al.*, 2020). It is left as a future work to achieve further unstable stratification experimentally.

## REFERENCES

Blass, A., Zhu, X., Verzicco, R., Lohse, D. & Stevens, R. J. A. M. 2020 Flow organization and heat transfer in turbulent wall sheared thermal convection. *J. Fluid Mech.* **897**, A22.

Etling, D. & Brown, R. A. 1993 Roll vortices in the planetary boundary layer: a review. *Boundary-Layer Meteorol.* **65**, 215–248.

Marusic, I., Monty, J. P., Hultmark, M. & Smits, A. J. 2013 On the logarithmic region in wall turbulence. *J. Fluid Mech.* **716**, R3–1–11.

Mizuno, Y., Yagi, T. & Mori, K. 2022 Momentum flux in turbulent boundary layers with weakly unstable stratification. *J. Phys. Soc. Jpn* **91**, 054402.

Monin, A. S. & Obukhov, A. M. 1954 Basic laws of turbu-

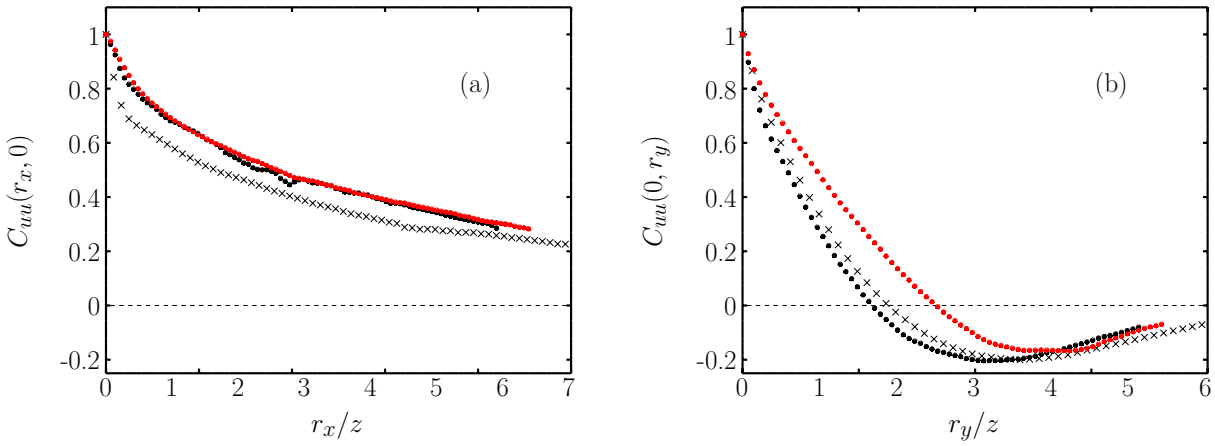


Figure 4. Correlation function (a) $C_{uu}(r_x,0)$ and (b) $C_{uu}(0,r_y)$ at $z/\delta \approx 0.15$. Symbols are as in Table 1.

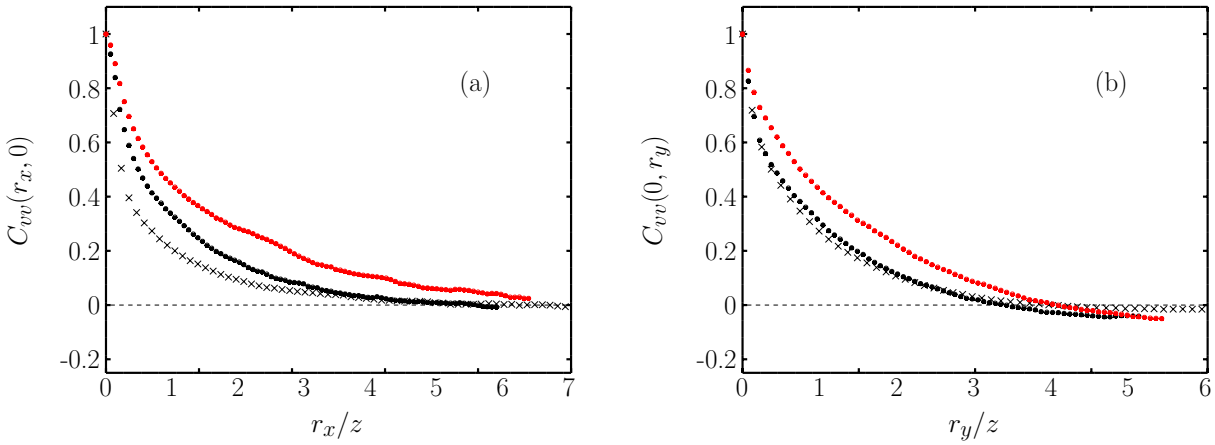


Figure 5. Same as figure 4, but for $C_{vv}$.

lent mixing in the atmosphere near the ground. *Trudy geofiz. inst. AN SSSR* **24**, 163–187.

Pirozzoli, S., Bernardini, M., Verzicco, R. & Orlandi, P. 2017 Mixed convection in turbulent channels with unstable stratification. *J. Fluid Mech.* **821**, 482–516.

Sillero, J. A., Jiménez, J. & Moser, R. D. 2013 One-point statistics for turbulent wall-bounded flows at Reynolds numbers up to $\delta^+ \approx 2000$. *Phys. Fluids* **25**, 105102.

Sillero, J. A., Jiménez, J. & Moser, R. D. 2014 Two-point statistics for turbulent boundary layers and channels at Reynolds numbers up to $\delta^+ \approx 2000$. *Phys. Fluids* **26**, 105109.

Townsend, A. 1976 *The Structure of Turbulent Shear Flow*, 2nd edn. Cambridge: Cambridge University Press.

Wyngaard, J. C. 2010 *Turbulence in the Atmosphere*. Cambridge: Cambridge University Press.